Quantum size effect and tunneling magnetoresistance in ferromagnetic-semiconductor quantum heterostructures

Shinobu Ohya,[1,2,*] Pham Nam Hai,[1] Yosuke Mizuno,[1] and Masaaki Tanaka[1,3,†]
[1]*Department of Electronic Engineering, The University of Tokyo, 7-3-1 Hongo, Bunkyo-ku, Tokyo 113-8656, Japan*
[2]*PRESTO Japan Science and Technology Agency, 4-1-8 Honcho, Kawaguchi, Saitama 332-0012, Japan*
[3]*SORST Japan Science and Technology Agency, 4-1-8 Honcho, Kawaguchi, Saitama 332-0012, Japan*
(Received 20 December 2006; revised manuscript received 19 February 2007; published 24 April 2007)

We report on the resonant tunneling effect and the increase of tunneling magnetoresistance induced by it in ferromagnetic-semiconductor GaMnAs quantum-well (QW) heterostructures. The resonant tunneling effect was observed when the GaMnAs QW thickness was from 3.8 to 20 nm, which indicates that highly coherent tunneling occurs in these heterostructures. The observed quantum levels of the GaMnAs QW were successfully explained by the valence-band $k \cdot p$ model and the p-d exchange interaction. It was also found that the Fermi level of the electrode injecting carriers is important to observe resonant tunneling in this system.

DOI: 10.1103/PhysRevB.75.155328 PACS number(s): 72.25.Dc, 73.40.Gk, 75.50.Pp, 85.75.Mm

I. INTRODUCTION

III-V-based ferromagnetic-semiconductor heterostructures containing GaMnAs are one of the best model systems to study spin-dependent transport phenomena, which can be used for future spintronic devices. Large tunneling magnetoresistance (TMR) of 75% (8.0 K)[1] and 290% (0.39 K)[2] were observed in the GaMnAs-based single-barrier heterostructures. Also, the GaMnAs-based quantum heterostructures are expected to realize new functions by combining a spin degree of freedom and the quantum-size effect (resonant tunneling effect).[3–11] For example, a very large enhancement of TMR up to ~800%[4] and to more than ~10^6%[3] is expected in GaMnAs-based resonant tunneling diode (RTD) structures. In magneto-optical measurements of the GaMnAs quantum well (QW), blueshifts of the magneto-optical spectra have been observed, suggesting the existence of the quantum-size effect in GaMnAs.[12,13] However, there are no reports on the clear observation of the resonant tunneling effect in ferromagnetic-semiconductor quantum heterostructures.[3,14,15] In the metal-based magnetic tunnel junctions (MTJs), the resonant tunneling effect and the TMR oscillation induced by it have been observed, though these phenomena appeared only when the QW thickness is extremely thin, less than 3 nm.[16,17] Comparing with these metal systems, the GaMnAs-based quantum heterostructures are fully epitaxial single crystals and have atomically flat interfaces, where highly coherent tunneling is expected. Therefore, this is a material system ideal for physical understanding of the spin-dependent resonant tunneling effect. Furthermore, it has good compatibility with III-V-based semiconductor devices and thus can lead to future three-terminal spin devices such as resonant tunneling spin transistors. Hence, it is a very important issue to observe resonant tunneling effect in III-V-based ferromagnetic heterostructures. In this paper, we report a successful detection of resonant tunneling effect and TMR increase induced by it in semiconductor heterostructures.

II. SAMPLE PREPARATION

Figure 1(a) shows the schematic device structure containing a GaMnAs QW confined by AlAs and AlGaAs barriers examined here. This heterostructure was grown by molecular beam epitaxy (MBE) with a layer structure from the surface to the substrate; $Ga_{0.95}Mn_{0.05}As$(20 nm)/ GaAs(1 nm)/ $Al_{0.5}Ga_{0.5}As$(4 nm)/ GaAs(1 nm)/ $Ga_{0.95}Mn_{0.05}As$ (d nm)/ GaAs(1 nm)/ AlAs(4 nm)/ Be-doped GaAs(100 nm) on a p-type GaAs(001) substrate, where the GaMnAs QW thickness d ranges from 3.8 to 20 nm. The Be concentration of the Be-doped GaAs (GaAs:Be) layer was 1×10^{18} cm^{-3}. The 1-nm-thick GaAs layers were inserted to prevent the Mn diffusion into the barrier layers and to smooth the surface. The GaAs:Be, AlAs, and the lowest GaAs spacer layers were grown at 600, 550, and 600 °C, respectively. The GaMnAs layers were grown at 225 °C, and GaAs/AlGaAs/GaAs layers below the top GaMnAs layer were grown at 205 °C. We grew four samples named A, B, C, and D. When growing sample A, we moved the in-plane position of the main shutter equipped in our MBE chamber in front of the sample surface during the growth of the GaMnAs QW, and changed d from 3.8 to 8.0 nm on the same sample wafer. In the growth of samples B–D, d was fixed at 12, 16, and 20 nm, respectively.

III. TUNNELING MAGNETORESISTANCE MEASUREMENTS

In order to carry out the tunneling magnetoresistance measurements, circular mesa diodes 200 μm in diameter were fabricated by chemical etching. We spin-coated an insulating negative resist on the sample, opened a contact hole 180 μm in diameter on the top of the mesa, and fabricated a metal electrode by evaporating Au on this surface. In the following measurements, the bias polarity is defined by the voltage of the top GaMnAs electrode with respect to the substrate. The schematic band diagrams when negative and positive biases V are applied to this structure are shown in Figs. 1(b) and 1(c), respectively. In this structure, TMR occurs by tunneling holes between the ferromagnetic GaMnAs top electrode and the ferromagnetic GaMnAs QW. The following tunneling transport measurements were carried out in a cryostat cooled at 2.6 K with a conventional two-terminal

1098-0121/2007/75(15)/155328(6) ©2007 The American Physical Society

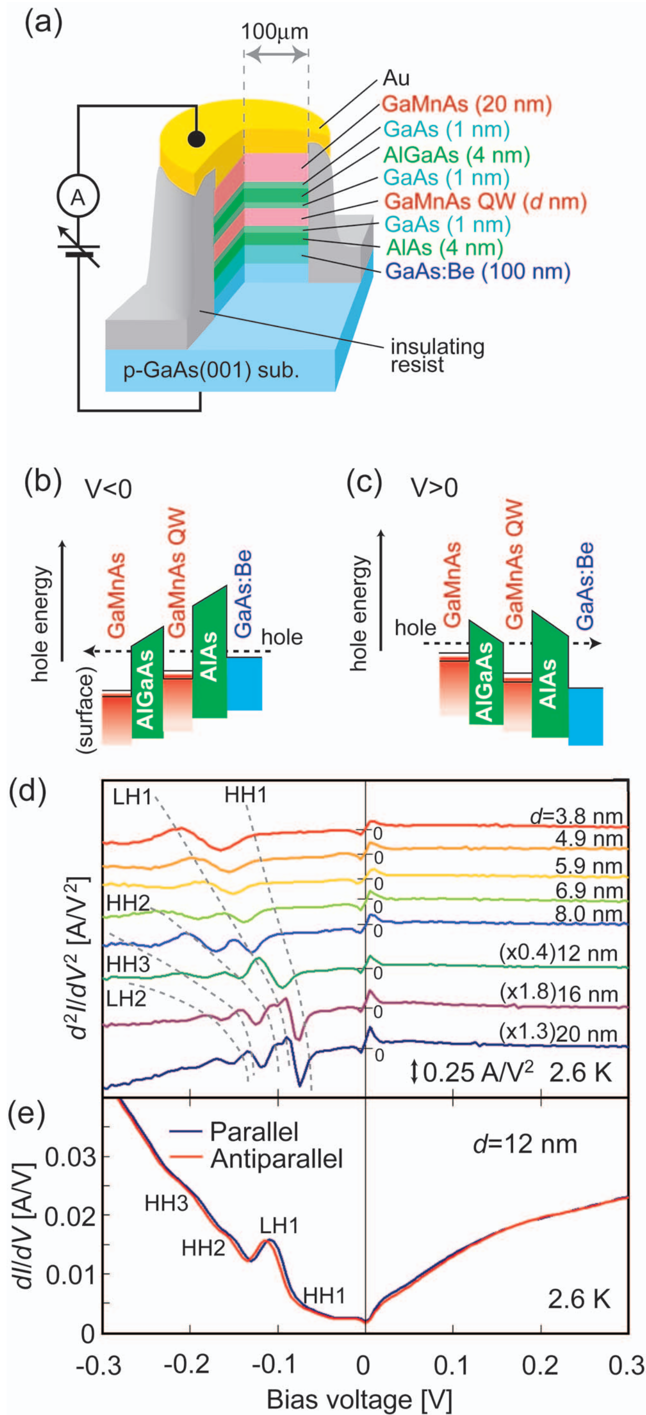

FIG. 1. (Color) (a) Schematic device structure of the $Ga_{0.95}Mn_{0.05}As$(20 nm) /GaAs(1 nm)/$Al_{0.5}Ga_{0.5}As$ (4 nm)/GaAs (1 nm)/$Ga_{0.95}Mn_{0.05}As$ (d nm)/GaAs (1 nm)/AlAs(4 nm)/GaAs: Be(100 nm) RTD junction examined in this study. (b) and (c) Schematic band diagrams of the RTD junction when the bias polarity is negative and positive, respectively. Here, the 1-nm-thick GaAs spacer layers are omitted for simplicity. (d) d^2I/dV^2-V characteristics of these RTD junctions with various QW thicknesses d in parallel magnetization at 2.6 K. Numbers in the parentheses express the magnification ratio for the vertical axis. (e) dI/dV-V characteristics of the junction with d=12 nm at 2.6 K in parallel (blue curve) and antiparallel (red curve) magnetization.

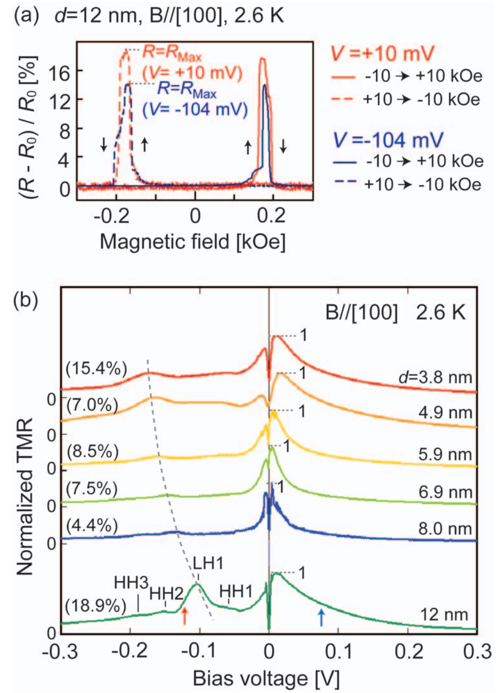

FIG. 2. (Color) (a) Tunneling magnetoresistance (TMR) curves [$(R-R_0)/R_0$ vs magnetic field] measured at 2.6 K on a junction with d=12 nm when the magnetic field was applied along the [100] axis in the plane, where R is the tunnel resistance and R_0 is the one at zero magnetic field. The measurements were carried out at constant bias voltages of 10 mV (red solid and broken curves) and −104 mV (blue solid and broken curves). Solid and broken curves were obtained by sweeping the field from −10 to 10 kOe and 10 to −10 kOe, respectively. The obtained TMR ratios, defined as $(R_{max}-R_0)/R_0$, in this RTD junction with d=12 nm at 10 mV and −104 mV were 18.9% and 14.1%, respectively. (b) Bias dependence of TMR in $Ga_{0.95}Mn_{0.05}As$(20 nm)/GaAs(1 nm)/$Al_{0.5}Ga_{0.5}As$(4 nm)/GaAs(1 nm)/$Ga_{0.95}Mn_{0.05}As$(d nm)/GaAs(1 nm)/AlAs(4 nm)/GaAs:Be(100 nm) RTD junctions with various QW thicknesses d when a magnetic field was applied in plane along the [100] direction at 2.6 K, where the TMR ratios are normalized by the maximum value of TMR in each curve shown in the parenthesis. These results were obtained by measuring TMR minor loops at various bias voltages and the TMR (estimated by the tunnel resistances in parallel and antiparallel magnetization states) at zero magnetic field was plotted as a function of bias voltage.

direct-current (dc) method. dI/dV-V and d^2I/dV^2-V characteristics were derived mathematically from the data of the I-V characteristics measured at every 5 mV. The results of the bias dependence of TMR were obtained from the data of I-V characteristics measured in parallel and antiparallel magnetizations. I-V characteristics in both parallel and antiparallel magnetizations were obtained at zero-magnetic field.

Figure 1(d) shows d^2I/dV^2-V characteristics of these junctions in parallel magnetization at 2.6 K. Sharp features near the zero bias are observed in all the curves with various d, corresponding to the zero-bias anomaly which is usually observed in GaMnAs-based heterostructures.[18] The most important feature in Fig. 1(d) is the oscillations whose peak voltages depend on d in the negative bias region of all the curves. With increasing d, these peaks shift to smaller volt-

ages and the period of the oscillation becomes short. Such oscillatory behavior has not been observed in GaMnAs-based single-barrier MTJs, indicating that these oscillations are induced by the resonant tunneling effect. The peaks HHn and LHn ($n=1, 2, 3, \ldots$) are assigned to resonant tunneling through the nth level of the heavy hole (HH) band and light hole (LH) band in the GaMnAs QW, respectively, as will be described later. Figure 1(e) shows the dI/dV-V curves of the junction with $d=12$ nm at 2.6 K in parallel (blue curve) and antiparallel (red curve) magnetization. These two curves are almost the same, but there is a little voltage shift which is most obvious at LH1.

TMR was clearly observed in the junctions with d from 3.8 to 12 nm. Figure 2(a) shows $(R-R_0)/R_0$ vs magnetic field characteristics (TMR curves) measured at 2.6 K on a junction with $d=12$ nm when the magnetic field was applied along the [100] axis in plane, where R is the tunnel resistance and R_0 is the one at zero magnetic field. These measurements were carried out at constant bias voltages of 10 mV (red solid and broken curves) and −104 mV (blue solid and broken curves). Solid and broken curves were obtained by sweeping the field from −10 to 10 kOe and 10 to −10 kOe, respectively. When the magnetic field H was swept from the positive saturation field down to negative (broken curves), the tunnel resistance R increased from the low-resistance (R_0) state to the high-resistance (R_{max}) state at around $H=-165$ Oe where the magnetization of one GaMnAs layer reversed and the magnetization configuration changed from parallel to antiparallel. Sweeping the field further to the negative direction, R decreased to the initial value at around $H=-200$ Oe where the magnetization of the other GaMnAs layer reversed and the magnetization configuration became parallel again. This is a typical TMR behavior usually observed in GaMnAs-based MTJs.[19–21] The obtained TMR ratios, defined as $(R_{max}-R_0)/R_0$, in this RTD junction with $d=12$ nm at 10 and −104 mV were 18.9% and 14.1%, respectively.

Figure 2(b) shows the bias dependence of the TMR ratio of these junctions at 2.6 K with a magnetic field applied in plane along the [100] direction, where the TMR ratios are normalized by the maximum value of TMR in each curve shown in the parenthesis. TMR oscillations can be seen in the negative bias region of all the curves. With increasing d, the TMR peaks (except for those near zero bias) shift to smaller voltages as is the case of the d^2I/dV^2-V characteristics shown in Fig. 1(d), which indicates that these TMR increases are induced by the resonant tunneling effect. Especially, a large TMR increase occurs at LH1, which is caused by the magnetization-dependent peak's shift at LH1 observed in the dI/dV-V characteristics shown in Fig. 1(e). Also, Fig. 2(b) indicates that the bias voltage of V_{half}, at which TMR is reduced by half, can be significantly increased by the resonant tunneling effect. In the negative-bias region of $d=12$ nm, $|V_{half}|$ was increased to 124 mV [shown by a red arrow in Fig. 2(b)] due to the TMR increase at LH1, whereas V_{half} in the positive bias was 76 mV [shown by a blue arrow in Fig. 2(b)]. This value is much higher than those of GaMnAs-based single-barrier structures which are usually around 50 mV.[2,22,23] On the other hand, the origin of the unusual sharp decrease of TMR near the zero bias is not clear, but it is probably partly due to the band offset of the GaMnAs QW as discussed below.

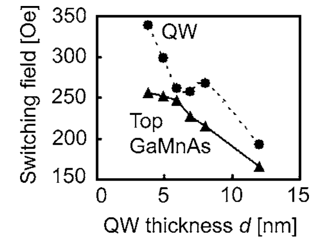

FIG. 3. Switching field (coercivity) as a function of d observed in the TMR curve of these RTD junctions at 2.6 K with a bias voltage of 10 mV and the magnetic field applied in plane along the [100] axis. The closed circles and triangles are the switching fields of the GaMnAs QW and the top GaMnAs electrode, respectively. Both of them tend to increase with decreasing d.

Figure 3 shows the switching field (coercivity) as a function of d observed in the TMR curve of these RTD junctions at 2.6 K with the bias voltage of 10 mV and the magnetic field applied in plane along the [100] axis. The closed circles and triangles are the switching fields of the GaMnAs QW and the top GaMnAs electrode, respectively. The switching field of the GaMnAs QW roughly tends to increase with decreasing d. (We note that a strong increase of coercivity by size reduction has been reported also in magnetic nanoclusters.[24]) The small peak at around $d=8$ nm is due to the degradation of the crystal quality (or of the surface flatness) of the GaMnAs QW, which can be seen also in Fig. 2(b), where the TMR ratio decreases with increasing d when d is less than 8 nm.[25] The reason why the switching field of the top GaMnAs layer also changes with d has not been clarified, yet, but it is probably due to the ferromagnetic coupling between the GaMnAs top electrode and the GaMnAs QW.

IV. COMPARISON WITH THEORETICAL CALCULATIONS

To understand the experimental results, we calculated the quantum levels of GaAs/$Al_{0.5}Ga_{0.5}As$(4 nm)/GaMnAs $\times$(d nm)/AlAs(4 nm)/GaAs using the transfer matrix method[26] with the valence-band 4×4 $k\cdot p$ Hamiltonian[27] and the p-d exchange Hamiltonian[28] for including the in-plane magnetization of the GaMnAs QW. The valence band lineup assumed in this calculation is shown in Fig. 4(a). We assumed that the splitting energy $\mathbf{\Delta}$ of the GaMnAs QW, which corresponds to the spin splitting energy for the LH valence band at the Γ point, is (3 meV, 0, 0) along the in-plane [100] direction parallel to the magnetic field applied in our experiments. The center energy of the spin-split valence band of the GaMnAs QW was set at 28 meV above the valence band of GaAs in terms of hole energy. (Later, we will discuss the validity of this energy position of the valence band of the GaMnAs QW.) Figure 4(b) shows the calculated result of the resonant-peak bias voltages for the heavy hole tunneling (red points and curves assigned to HHn) and the light hole tunneling (blue points and curves assigned to LHn) at $k_{\parallel}=0$,

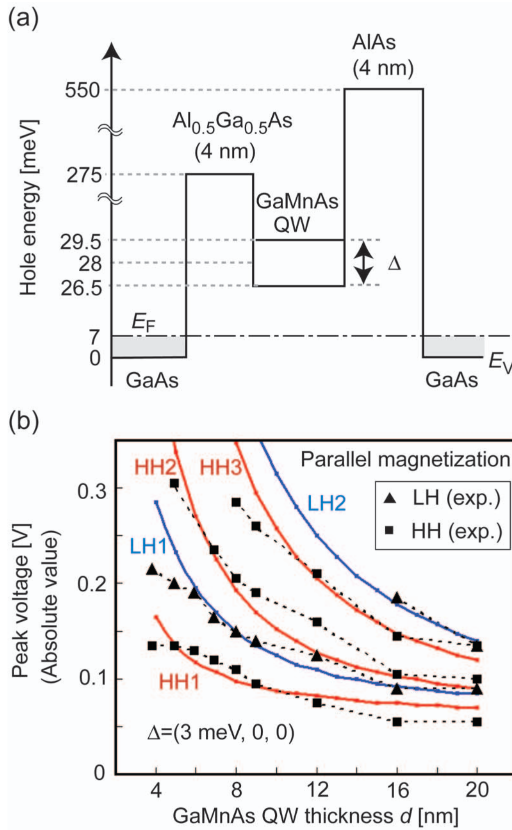

FIG. 4. (Color) (a) Valence-band lineup assumed in our calculation of the quantum levels in $GaAs/Al_{0.5}Ga_{0.5}As$ (4 nm)/GaMnAs(d nm)/AlAs(4 nm)/GaAs. E_F, E_V, and Δ mean the Fermi level, the valence band edge, and the spin-splitting energy of the light-hole band of the GaMnAs QW at the Γ point, respectively. (b) Calculated and experimentally obtained resonant peak voltage vs the GaMnAs QW thickness d. The black solid rectangles and triangles denote the experimentally obtained resonant-peak voltages assigned as HH and LH quantum levels in the d^2I/dV^2-V characteristics of $Ga_{0.95}Mn_{0.05}As$(20 nm)/GaAs(1 nm)/$Al_{0.5}Ga_{0.5}As$(4 nm)/GaAs(1 nm)/$Ga_{0.95}Mn_{0.05}As$(d nm)/GaAs(1 nm)/AlAs (4 nm)/GaAs:Be(100 nm) RTD junctions in parallel magnetization, respectively. Here, these voltages are expressed in the absolute values. The small red and blue points (curves) denote the calculated resonant voltages of HH and LH, respectively. The quantum levels of LH1 and LH2 are spin-split by the in-plane magnetization introduced by the p-d exchange Hamiltonian. The calculated voltages of the LH quantum levels shown in this figure are those in parallel magnetization.

where $k_{\parallel}$ is the wave vector parallel to the film plane. These resonant peak bias voltages were derived by multiplying the calculated energy values of the quantum levels by 2.5 [ideally, this value is 2 (Ref. 29)] for better fit, which means that 20% of the applied bias voltage is consumed in the electrodes. Since the heavy hole spins are oriented along the tunneling direction and the p-d exchange Hamiltonian is proportional to $\mathbf{s}\cdot\mathbf{S}$, the quantum levels of HH are not spin split but those of LH are split by the in-plane magnetization,[30] where $\mathbf{s}$ and $\mathbf{S}$ are spins of the carrier and the Mn atom, respectively. Holes tunnel through the lower and upper states of the spin-split LH quantum levels in parallel and in antiparallel magnetization, respectively. The calculated voltages of the LH quantum levels shown in Fig. 4(b) are those in parallel magnetization.

Figure 4(b) also shows the experimental peak voltages assigned to HH and LH quantum levels observed in the d^2I/dV^2-V curves in parallel magnetization by black solid rectangles and triangles, respectively. Here, the peak voltages are expressed in the absolute values. Although there is a little deviation between the experimental and calculated results, the experimental results are well-fitted by the present model. Possible origins of these deviations are considered as follows. When d is thinner than 5 nm, Mn diffusion from the GaMnAs QW layer to the adjacent GaAs spacer layer yields lowering of the resonant tunneling energy. The deviations may also come from the point defects incorporated into GaMnAs such as Mn interstitials[31] and As antisite defects,[32] whose concentrations are very sensitive to the growth condition of GaMnAs.[33] These defects can influence the spin-splitting energy, band offset, and strain, leading to such deviations. We note that the spin-splitting energy (3 meV, 0, 0) is consistent with our results of the temperature dependence of TMR, where TMR disappeared at around 20 K when increasing temperature.[34,35] Also, this spin-splitting energy can well-explain the quantity of the peak voltage shift of 7(±2) mV observed in the dI/dV-V curves with parallel and antiparallel magnetizations at LH1 shown in Fig. 1(e) (i.e., $7\approx 3\times 2.5$). Our result that the quantum levels of the GaMnAs QW can be described by the spin-split valence-band model indicates that the tunneling phenomena through the GaMnAs QW are strongly associated with the valence-band feature.

V. DISCUSSION

In our experiment, the resonant peaks were observed only in the negative bias region, where holes are injected from the GaAs:Be layer to the GaMnAs QW. We think that it is attributed to the difference of the Fermi energy E_F between the top GaMnAs and the bottom GaAs:Be electrodes.[34] Figure 5(a) shows the schematic valence-band diagrams of the GaMnAs electrode (left graph) and the hole subband structure of AlAs(1 nm)/GaAs QW (5 nm)/AlAs(1 nm) (right graph) calculated by the $k\cdot p$ model. For simplicity, we ignored the spin splitting and used an AlAs barrier instead of AlGaAs. Also, a single band is assumed in the GaMnAs electrode. GaMnAs has a large hole concentration of the order of 10^{20} to 10^{21} cm^{-3}, thus a large E_F around 200 meV. (Here, we assumed that E_F exists in the valence band. Even if E_F exists in the impurity band as mentioned in the next paragraph, the result of this discussion does not change.[36]) Considering the freedom in the k_z direction of holes in the bulk GaMnAs electrode, this high E_F means that the holes occupy a wide $k_{\parallel}$ region. Now, we consider that holes are injected to the GaMnAs QW from the GaMnAs electrode whose energy is increased by the bias voltage, as shown in Fig. 5(a). If $k_{\parallel}$ is conserved during tunneling, holes are injected to the subbands of the GaMnAs QW within the gray region. The circular points correspond to the states of the maximum or minimum energies in each subband in the gray

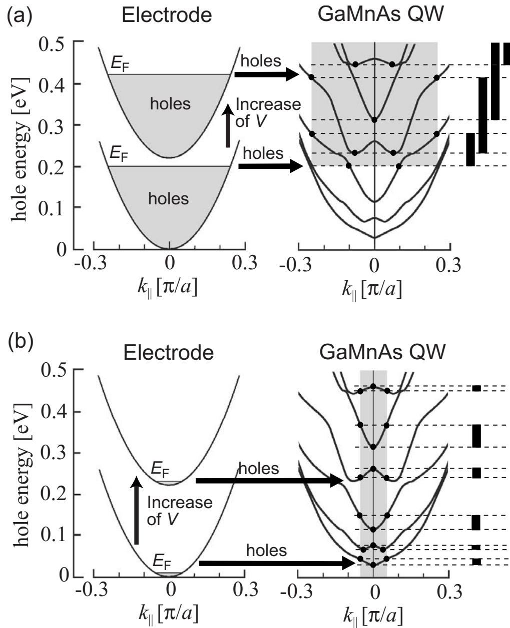

FIG. 5. (a) Schematic valence-band diagrams of the GaMnAs electrode (left graph) and the hole subband structure of AlAs(1 nm)/GaAs QW (5 nm)/AlAs(1 nm) (right graph) calculated by the $k\cdot p$ model. For simplicity, we ignored the spin splitting and used an AlAs barrier instead of AlGaAs, respectively. Also, a single band is assumed in the electrode. E_F is assumed to be 200 meV. The gray regions in the GaMnAs QW bandstructure correspond to the $k_\parallel$ regions where tunneling can occur, and the black bands on the right side are corresponding energy regions. The circular points correspond to the states of the maximum and minimum energies in each subband within the gray region. The broken lines are maximum and minimum energies of each subband within the gray region. (b) The case when holes are injected from the electrode with a small hole concentration like GaAs:Be. E_F is assumed to be 7 meV.

region. The black bands shown on the right side are the energy regions corresponding to these subbands in the gray region. We can see that these energy regions of the subbands are energetically overlapped, thus these subbands cannot be detected separately in tunneling transport measurements. On the other hand, if carriers are injected from GaAs:Be with a smaller carrier concentration of 1×10^{18} cm^{-3} whose Fermi level is estimated to be about 7 meV, the tunneling occurs only within a small $k_\parallel$ region. Figure 5(b) shows the schematic valence-band diagrams of the GaAs:Be electrode (left graph) and the subbands in the GaMnAs QW (right graph). When carriers are injected from such an electrode with a small Fermi level, these carriers are injected into the gray regions and black bands of the GaMnAs QW in Fig. 5(b), where these energy regions are energetically separated. Therefore, the resonant peaks are observed only in the negative bias region. Our result indicates that electrodes with a low carrier concentration are appropriate for clear detection of the resonant tunneling effect in GaMnAs QW heterostructures.

Here, we discuss the validity of the energy position of the GaMnAs QW assumed in our calculation. As can be seen in Fig. 4(a), the energy of the valence-band bottom (or of the HH1 level) of the GaMnAs QW is higher than E_F ($\approx$7 meV). This means that there are almost no holes in the GaMnAs QW when the bias voltage is small. Under the general concept of the carrier-mediated ferromagnetism where the ferromagnetism of GaMnAs is induced by the valence-band holes,[37] the GaMnAs QW in our RTD devices would not become ferromagnetic because there is no holes in its valence band. In our experiment, however, the GaMnAs QW is ferromagnetic because TMR was observed even when the bias voltage is small. At present, this discrepancy is not perfectly understood, but we think it might be partly due to the low Curie temperature of the GaMnAs QW in our RTD samples ($\sim$20 K). It is well-known that the ferromagnetic GaMnAs films with a low Curie temperature often show strong insulating behavior even when the temperature is below its Curie temperature.[38] In this case, mobile valence-band holes are not likely to exist there. Recently, Burch *et al.*[39] indicated that E_F of GaMnAs exists not in the valence band but in the impurity band in the band gap of GaMnAs by measuring the infrared optical spectroscopy. Although there is a little difference of the energy positions of E_F obtained in their results (around 100–200 meV from the valence band) and in our results (28−7=21 meV from the valence band of GaMnAs), their results seem to qualitatively support our present understanding of the quantum levels in the GaMnAs QW. Note also that E_F of GaMnAs strongly depends on the growth conditions.

In our experiment, a very large TMR enhancement as predicted in the theories[3,4] was not obtained. The possible reason of this is the small spin splitting (3 meV) obtained in the GaMnAs QW of our RTD devices. If a GaMnAs QW with a larger spin-splitting energy can be obtained by using a better growth condition (i.e., more appropriate growth temperature and arsenic pressure) where the concentration of the interstitial Mn defects is minimized, a larger TMR enhancement will be obtained. Also, if a high-quality epitaxial QW composed of a single-crystal ferromagnetic metal with larger spin splitting can be obtained, TMR will be largely enhanced.

VI. SUMMARY

We have observed the resonant tunneling effect and TMR increase induced by it in GaMnAs-QW double-barrier heterostructures with the QW thickness from 3.8 to 20 nm, indicating highly coherent tunneling occurs in these heterostructures. The observed quantum levels of the GaMnAs QW were successfully explained by the coherent tunneling model with the valence-band $k\cdot p$ model and the p-d exchange interaction. It was also found that electrodes with a low carrier concentration are appropriate for clear detection of the resonant tunneling effect in this system.

ACKNOWLEDGMENTS

This work was partly supported by PRESTO/SORST of JST, Grant-in-Aids for Scientific Research, IT Program of RR2002 of MEXT, and Kurata-Memorial Hitachi Science & Technology Foundation.

*Electronic address: ohya@cryst.t.u-tokyo.ac.jp
†Electronic address: masaaki@ee.t.u-tokyo.ac.jp

[1] M. Tanaka and Y. Higo, Phys. Rev. Lett. **87**, 026602 (2001).
[2] D. Chiba, F. Matsukura, and H. Ohno, Physica E (Amsterdam) **21**, 966 (2004).
[3] T. Hayashi, M. Tanaka, and A. Asamitsu, J. Appl. Phys. **87**, 4673 (2000).
[4] A. G. Petukhov, A. N. Chantis, and D. O. Demchenko, Phys. Rev. Lett. **89**, 107205 (2002).
[5] S. S. Makler, M. A. Boselli, J. Weberszpil, X. F. Wang, and I. C. da Cunha Lima, Physica B **320**, 396 (2002).
[6] F. Giazotto, F. Taddei, R. Fazio, and F. Beltram, Appl. Phys. Lett. **82**, 2449 (2003).
[7] T. Uemura, T. Marukame, and M. Yamamoto, IEEE Trans. Magn. **39**, 2809 (2003).
[8] I. Vurgaftman and J. R. Meyer, Appl. Phys. Lett. **82**, 2296 (2003).
[9] H.-B. Wu, K. Chang, J.-B. Xia, and F. M. Peeters, J. Supercond. **16**, 279 (2003).
[10] N. Lebedeva and P. Kuivalainen, Phys. Status Solidi B **242**, 1660 (2005).
[11] S. Ganguly, L. F. Register, S. Banerjee, and A. H. MacDonald, Phys. Rev. B **71**, 245306 (2006).
[12] H. Shimizu and M. Tanaka, J. Appl. Phys. **91**, 7487 (2002).
[13] A. Oiwa, R. Moriya, Y. Kashimura, and H. Munekata, J. Magn. Magn. Mater. **272-276**, 2016 (2004).
[14] R. Mattana, J.-M. George, H. Jaffrès, F. Nguyen Van Dau, A. Fert, B. Lépine, A. Guivarc'h, and G. Jézéquel, Phys. Rev. Lett. **90**, 166601 (2003).
[15] S. Ohya, P. N. Hai, and M. Tanaka, Appl. Phys. Lett. **87**, 012105 (2005).
[16] T. Nozaki, N. Tezuka, and K. Inomata, Phys. Rev. Lett. **96**, 027208 (2006).
[17] S. Yuasa, T. Nagahama, and Y. Suzuki, Science **297**, 234 (2002).
[18] S. H. Chun, S. J. Potashnik, K. C. Ku, P. Schiffer, and N. Samarth, Phys. Rev. B **66**, 100408(R) (2002).
[19] Y. Higo, H. Shimizu, and M. Tanaka, J. Appl. Phys. **89**, 6745 (2001).
[20] We note that the TMR ratio of our RTD devices maintained the positive values with any angles of in-plane magnetic fields. Also, the same TMR ratios were obtained when the magnetic field is applied in the in-plane [100] and [010] axes. Thus this change of the tunnel resistance observed here is attributed to TMR not to tunneling anisotropic magnetoresistance (TAMR) (Ref. 21).
[21] C. Rüster, C. Gould, T. Jungwirth, J. Sinova, G. M. Schott, R. Giraud, K. Brunner, G. Schmidt, and L. W. Molenkamp, Phys. Rev. Lett. **94**, 027203 (2005).
[22] R. Mattana, M. Elsen, J.-M. George, H. Jaffrès, F. Nguyen Van Dau, A. Fert, M. F. Wyczisk, J. Olivier, P. Galtier, B. Lépine, A. Guivarc'h, and G. Jézéquel, Phys. Rev. B **71**, 075206 (2005).
[23] M. Elsen, O. Boulle, J.-M. George, H. Jaffrès, R. Mattana, V. Cros, A. Fert, A. Lemaitre, R. Giraud, and G. Faini, Phys. Rev. B **73**, 035303 (2006).
[24] J. Jin, S. Ohkoshi, and K. Hashimoto, Adv. Mater. (Weinheim, Ger.) **16**, 48 (2004).
[25] Because the angles of the direction of the Ga, Mn, and As fluxes are slightly different in the MBE chamber, there is a small region which is not covered by one of the fluxes on the sample surface in the vicinity of the edge of the main shutter. This is the main reason for the degradation of the crystal quality (or of the surface flatness) of the GaMnAs QW fabricated with moving the main shutter.
[26] R. Wessel and M. Altarelli, Phys. Rev. B **39**, 12802 (1989).
[27] J. M. Luttinger and W. Kohn, Phys. Rev. **97**, 869 (1955).
[28] T. Dietl, H. Ohno, and F. Matsukura, Phys. Rev. B **63**, 195205 (2001).
[29] In the ideal RTD structure, the same voltage drops occur at the two barriers and no voltage drops occur in other regions (electrodes and QW), thus the ideal multiple number is 2.
[30] M. Sawicki, F. Matsukura, A. Idziaszek, T. Dietl, G. M. Schott, C. Ruester, C. Gould, G. Karczewski, G. Schmidt, and L. W. Molenkamp, Phys. Rev. B **70**, 245325 (2004).
[31] K. M. Yu, W. Walukiewicz, T. Wojtowicz, I. Kuryliszyn, X. Liu, Y. Sasaki, and J. K. Furdyna, Phys. Rev. B **65**, 201303(R) (2002).
[32] B. Grandidier, J. P. Nys, C. Delerue, D. Stiévenard, Y. Higo, and M. Tanaka, Appl. Phys. Lett. **77**, 4001 (2000).
[33] H. Shimizu, T. Hayashi, T. Nishinaga, and M. Tanaka, Appl. Phys. Lett. **74**, 398 (1999).
[34] H. Ohno, N. Akiba, F. Matsukura, A. Shen, K. Ohtani, and Y. Ohno, Appl. Phys. Lett. **73**, 363 (1998).
[35] In Ref. 34, it was reported that the spin-splitting energy of the HH valence band of GaMnAs with a Curie temperature of ~70 K was estimated to be 44 meV. If we simply assume the spin-splitting energy of HH is three times larger than that of LH, the spin-splitting energy of the LH valence band in their sample is ~15 meV. The Curie temperature of the GaMnAs layers in our heterostructures is estimated to be around 20 K, thus the value of the spin-splitting energy of 3 meV of our GaMnAs layers is reasonable (i.e., $3 \approx 15 \times 20/70$).
[36] Because the effective mass of the impurity-band holes is very large, the tunneling occurs in the wide range of the $k_{\parallel}$ region when holes are injected from the impurity band of GaMnAs. Thus the same discussion is possible.
[37] T. Dietl, H. Ohno, F. Matsukura, J. Cibert, and D. Ferrand, Science **287**, 1019 (2000).
[38] A. Oiwa, S. Katsumoto, A. Endo, M. Hirasawa, Y. Iye, H. Ohno, F. Matsukura, A. Shen, and Y. Sugawara, Solid State Commun. **103**, 209 (1997).
[39] K. S. Burch, D. B. Shrekenhamer, E. J. Singley, J. Stephens, B. L. Sheu, R. K. Kawakami, P. Schiffer, N. Samarth, D. D. Awschalom, and D. N. Basov, Phys. Rev. Lett. **97**, 087208 (2006).